

Diffusion-Controlled and “Diffusionless” Crystal Growth near the Glass Transition: Relation between Liquid Dynamics and Growth Kinetics of Seven ROY Polymorphs

Ye Sun,^a Hanmi Xi,^b M. D. Ediger,^a Ranko Richert^c, Lian Yu^{b,a}*

^a University of Wisconsin – Madison, Department of Chemistry, Madison, WI 53706. ^b University of Wisconsin – Madison, School of Pharmacy, Madison, WI 53705. ^c Department of Chemistry and Biochemistry, Arizona State University, Tempe, Arizona 85287.

AUTHOR EMAIL ADDRESS: lyu@pharmacy.wisc.edu

TITLE RUNNING HEAD. Diffusion-Controlled and “Diffusionless” Crystal Growth near T_g

CORRESPONDING AUTHOR FOOTNOTE. Tel: (608) 263 2263. email: lyu@pharmacy.wisc.edu

ABSTRACT. The liquid dynamics of 5-methyl-2-[(2-nitrophenyl)amino]-3-thiophenecarbonitrile, named ROY for its red, orange, and yellow crystal polymorphs, was characterized by dielectric spectroscopy and differential scanning calorimetry to study the fast, diffusionless growth of some but not all of its polymorphs. ROY was found to be a typical fragile organic liquid. Its α relaxation process has time-temperature superposition symmetry across the viscous range ($\tau_\alpha = 100$ s - 100 ns) with the width of the relaxation peak characterized by a constant β_{KWW} of 0.73. No secondary relaxation peak was observed, even with glasses made by fast quenching. For the polymorphs not showing fast growth

in the glassy state, the growth rate has a power-law relation with τ_α , $u \propto \tau_\alpha^{-\xi}$, where $\xi \approx 0.7$. For the polymorphs showing fast crystal growth in the glassy state, the growth is so fast near and below the glass transition temperature T_g that during one τ_α , thousands of molecular layers can be added to the crystalline phase. In the glassy state, this mode of growth slows slightly over time. This slowdown is not readily explained by the effect of physical aging on the thermodynamic driving force of crystallization, the glass vapor pressure, or the rate of structural relaxation.

INTRODUCTION

If cooled without crystallizing, a liquid eventually solidifies to a glass or amorphous solid at the so-called glass transition temperature T_g . For many applications, glasses are advantageous over crystals.¹ Although the solidity of glasses might suggest stability against crystallization, glasses can crystallize, sometimes surprisingly fast. Understanding their crystallization is relevant to developing amorphous materials and to elucidating the link between crystallization kinetics and molecular mobility.

A remarkable property of crystallization in organic liquids is that a new, fast mode of crystal growth may emerge near T_g and continue deep in the glassy state.^{2,3} Greet and Turnbull were apparently the first to notice the phenomenon in 1967.² By comparing the observed crystal growth rates with those calculated on the assumption that crystals cannot grow faster than molecules can diffuse, they found that crystal growth in liquid *o*-terphenyl (OTP) is accurately described as diffusion-controlled over a wide range of temperature above T_g , but is orders of magnitude too fast near and below T_g . In 1995, Oguni and coworkers independently observed the phenomenon³ and reported that the fast growth is abruptly activated near T_g on cooling and disappears at the same temperature on heating. The data now available on the dynamics of liquid OTP provide other contexts for evaluating this fast mode of crystal growth: at 246 K (T_g), it takes 50 ms for the crystalline phase to add one layer of molecules,³ but it requires at least 100 times longer for an average molecule to diffuse the same distance⁴ or reorient substantially, or for the liquid to undergo substantial structural relaxation.⁵ These properties make it appropriate to describe the onset of the fast growth mode as a transition from diffusion-controlled to “diffusionless” crystal

growth, with the diffusion here understood as bulk diffusion. Many liquids are now known to show this transition, all of which are organic glass formers.^{6,7,8,9} For convenience, we shall call the fast crystal growth “GC” (glass-crystal) for it is observed deep in the glassy state. The fact that crystals can grow in the absence of significant bulk diffusion is in conflict with the established view that the kinetic barrier for crystal growth in a liquid is similar to that for diffusion.^{10,11,12,13,14}

Recent studies have revealed new features of GC growth. Despite its abrupt emergence near T_g , the GC mode can persist above T_g (up to $1.15 T_g$) in the form of fast-growing fibers.^{8,15} It appears that GC growth is fully activated only at sufficiently low temperatures; it is disrupted (though not eliminated) by the onset of liquid-like mobility. Sun et al. reported that GC growth exists only for certain crystal structures.¹⁶ By studying the liquid of 5-methyl-2-[(2-nitrophenyl) amino]-3-thiophenecarbonitrile, named ROY for its many red, orange, and yellow crystal polymorphs,^{17,18} they observed that three polymorphs do not show GC growth, whereas four others do, with the latter having higher densities and more isotropic molecular packing.

This work was carried out to characterize the dynamics of liquid ROY so that the crystal growth kinetics of the various polymorphs can be accurately described in reference to motions in the liquid and glassy state. Measurements by dielectric spectroscopy revealed that ROY is a typical fragile organic liquid. For the polymorphs not showing GC growth, a power-law relation exists between the growth rate u and the primary relaxation time τ_α , $u \propto \tau_\alpha^{-\xi}$, where $\xi \approx 0.7$, as found for other systems showing diffusion-controlled crystal growth; their absolute growth rates u are such that the time for the crystalline phase to gain one molecular layer is substantially longer than τ_α . In contrast, the polymorphs showing the GC mode grow so much faster near and below T_g that during one τ_α , many molecular layers are added to the crystalline phase and the growth rate “decouples” from τ_α to a greater extent. These results confirm that depending on their crystal structures, different polymorphs of ROY can grow from the same liquid both in a diffusion-limited process and free from diffusion control.

This work also examined whether crystal growth slows over time in glassy ROY, as recently observed for glassy OTP.¹⁵ This property is of interest for testing the various explanations for GC growth. This

work found a similar slowdown of crystal growth: in 10 hours at 248 K ($T_g - 11$ K), the crystal growth rate of polymorph YT04 decreases by ca. 13 %. Under the same condition, the glass relaxation reduces the enthalpic fictive temperature by 7 K and increases the structural relaxation time by an estimated 23 times. As in the case of OTP, the slowdown of GC growth over time is not readily explained by the effect of physical aging on the thermodynamic driving force of crystallization, the glass vapor pressure, or the primary structural relaxation.

EXPERIMENTAL SECTION

Samples for dielectric measurements were prepared by melting ROY onto a 30 mm diameter polished stainless steel disk, adding four strips of Teflon as 25 μm spacers, and covering the sample with a second electrode of 20 mm diameter. With this capacitor mounted in the sample holder, ROY was reheated to 403 K for 8 minutes and cooled to the measurement temperature at a rate of ca. 15 K/min. A nitrogen-gas cryostat with a Novocontrol Quatro controller was used to control the sample temperature. The stability of the temperature reading was better than 0.05 K. To obtain a rapidly quenched sample, the above preparation was repeated with brass electrodes and with the capacitor assembly being immersed in liquid nitrogen, which resulted in a cooling rate of 490 K/min. The sample was then transferred to the cryostat (pre-cooled to 120 K) under N_2 atmosphere.

Frequency-dependent dielectric permittivity ϵ' and loss ϵ'' were measured using the frequency response analyzer Solartron SI-1260 equipped with a Mestec DM-1360 transimpedance amplifier. Calibration was performed by measuring the capacitor with $C_{\text{geo}} = 110$ pF with a 25 μm thick Teflon sheet ($\epsilon_s = 2.0$) as loss free reference. Stated values were corrected for the ≈ 20 % volume fraction of the Teflon spacer material. Quantitative analyses of the loss curves were based upon the Havriliak-Negami (HN) type dielectric function plus a term for dc-conductivity,¹⁹

$$\epsilon^*(\omega) = \epsilon'(\omega) - i\epsilon''(\omega) = \epsilon_\infty + \frac{\epsilon_s - \epsilon_\infty}{[1 + (i\omega\tau_{HN})^\alpha]^\gamma} + \frac{\sigma_{dc}}{i\omega\epsilon_0}, \quad (1)$$

where ϵ_∞ is the dielectric constant in the high frequency limit and $\Delta\epsilon = \epsilon_s - \epsilon_\infty$ is the relaxation strength with ϵ_s being the static dielectric constant. The exponents α and γ ($0 < \alpha, \alpha\gamma \leq 1$) quantify the symmetric and asymmetric broadening, respectively. The value of σ_{dc} quantifies the level of dc-conductivity. For comparison with other systems, it is of interest to obtain the Kohlrausch-Williams-Watts (KWW) parameters for liquid ROY. The KWW function often describes equivalent relaxation behavior as the HN function, with the HN fit typically used for frequency-domain data and the KWW fit for time-domain data. In this work, the KWW stretching exponent is derived from the HN parameters α and γ via the relation $\beta_{KWW} = (\alpha\gamma)^{0.81}$.²⁰

Differential Scanning Calorimetry (DSC) was conducted with a TA Instruments Q2000 under N₂ purge (50 ml/min). The temperature of the DSC was calibrated against the melting of indium and ice. To measure the kinetics of enthalpy relaxation of a ROY glass, ca. 3 mg of ROY crystals were packed in a crimped aluminum pan, which provided complete contact with the sample (no head space or free surface), melted at 403 K for 5 min, and cooled at 40 K/min to 278 K ($T_g + 19$ K) and at 10 K/min to 248 K ($T_g - 11$ K), and aged at 248 K for a time ranging from 0 to 36000 s. After each aging step, the sample was cooled at 10 K/min to 203 K and heated at 10 K/min to 403 K to measure its heat capacity C_p to be used for calculating the fictive temperature of the aged glass.²¹ By DSC, the onset temperature of the glass transition is 261 K (measured by heating at 10 K/min, following cooling at 10 K/min). This calorimetric T_g is in acceptable agreement with the “kinetic” T_g of 259 K obtained by dielectric spectroscopy, which is defined as the temperature at which the average primary relaxation time $\langle \tau \rangle$ is 100 s. The latter value is used as T_g throughout this paper.

Modulated-DSC (MDSC) was used to measure the absolute values of C_p . For this measurement, 10 mg of ROY liquid was sealed in a hermetic pan and its temperature was modulated by ± 0.25 K every 60 s about 283 K. The C_p of the sample was obtained from the reversing C_p signal of the MDSC after calibration against a sapphire standard. The C_p of liquid ROY was found to be 1.57 J/(g K) at 283 K

(the error in C_p is estimated to be smaller than 5 %). All the C_p curves obtained from heating at 10 K/min were vertically shifted to this value.

To observe the growth of polymorph YT04 in a ROY liquid or glass, 3 mg of ROY crystals were melted between two round cover glasses (15 mm diameter) on a hot/cold stage (Linkam THMS 600) at 403 K for 5 min and cooled at 20 K/min to 295 K. The resulting liquid film was 10 – 15 μm thick. The liquid was maintained at 295 K until polymorph Y04 nucleated;¹⁸ the temperature was lowered to 265 K to allow polymorph YT04 to “cross-nucleate” on Y04.¹⁶ The crystal growth rate was measured from the distance by which a crystal front advanced into the melt as a function of time (see Figure 5 for typical data), with the aid of a microscope (Olympus BH2-UMA). This work examined the time dependence of crystal growth rate of YT04 at 265 K ($T_g + 6$ K) and 248 K ($T_g - 11$ K). At each temperature, the growth yielded compact spherulites and the radial growth rate was measured. At 265 K, we typically waited for 15 min for YT04 to nucleate on Y04 and another 15 min for YT04 to develop a smooth, steady state growth front before recording the growth. The growth at 265 K was tracked up to 8 hours. At 248 K, the YT04 crystal growth was first established at 265 K as described above, the temperature was lowered to 248 K, and the growth was monitored at 248 K up to 30 hours.

Apart from real-time measurements, the method of growth rings was used to measure crystal growth rates. This method relies on the distinguishable textures of crystals grown at different temperatures (see Figure 6a for an example). To carry out this method, a cover-glass sample was prepared as described above and kept at 295 K long enough for polymorph Y04 to crystallize, which would later serve to cross-nucleate polymorph YT04. The sample was then placed in the DSC cell waiting at 265 K. To study crystal growth at 265 K, the sample was kept at 265 K for a progressively longer time: 5400, 7200, 14400, and 28800 s. Between two holding periods, the sample spent 1200 s at 254 K to grow a “marker” ring. The first holding period (5400 s at 265 K) was to initiate the crystallization of YT04 on Y04. To study crystal growth at 248 K, the sample was first kept at 265 K for 14400 s to establish the growth of YT04, and then at 248 K for a progressively longer time: 14400, 28800, and 57600 s. Between two holding periods, the sample spent 5400 s at 265 K to grow a “marker” ring and to erase the

effect of glass aging. On completion of the temperature program, the sample was removed from the DSC cell and the widths of the growth rings were measured under the microscope. From each growth ring, the average growth rate was calculated for the corresponding time interval. From the growth rings developed over increasingly longer times, namely, 0 to t_1 , 0 to t_2 , 0 to t_3 , etc., with $t_1 < t_2 < t_3 \dots$, the average growth rates were calculated for consecutive time intervals (0 to t_1 , t_1 to t_2 , t_2 to t_3 , etc.).

RESULTS

Dielectric Relaxation. The dielectric permittivity ϵ' and loss ϵ'' of liquid ROY were measured between 175 and 320 K. The high-frequency dielectric constant is $\epsilon_\infty = 4.6$ and the static dielectric constant is $\epsilon_s = 50.4$ at T_g . The relatively high dielectric constant of liquid ROY is consistent with its high molecular dipole moment (6 - 8 D by ab initio calculations for its crystal conformers^{17,18}). Figure 1 shows the loss curves $\epsilon''(\nu)$ in the α relaxation regime. The bottom panel shows data obtained during heating in steps of 2 K with a sample quenched from 403 K to 256 K at ca. 15 K/min. In this sample,

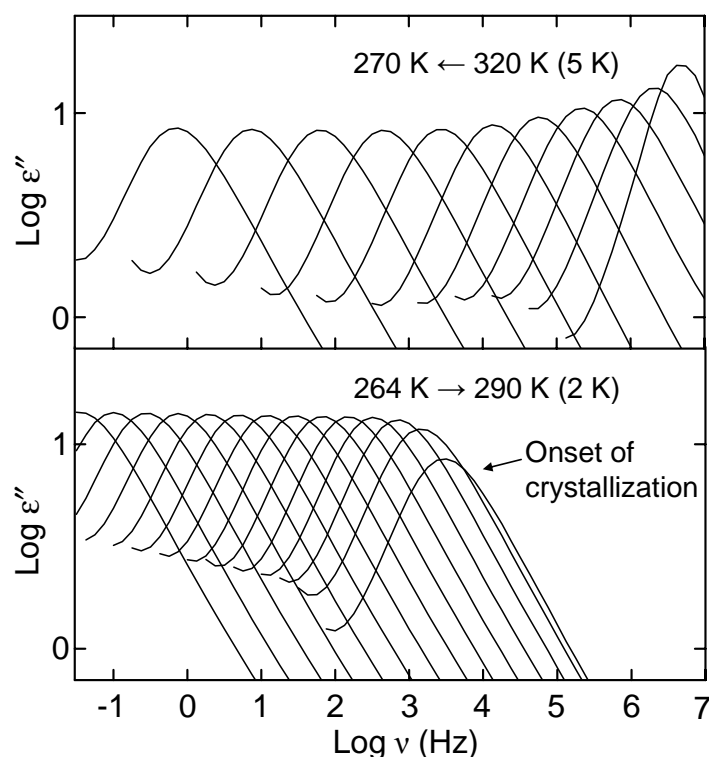


Figure 1. Dielectric loss ϵ'' versus ν at various temperatures. Top: Data obtained during cooling from 320 K to 270 K (right to left) in steps of 5 K. Bottom: Data obtained during heating from 256 K to 290 K (left to right) in steps of 2 K. The low-frequency DC conductivity wing of each spectrum was removed for clarity.

crystallization occurred near 286 K ($T_g + 27$ K), causing a decrease of liquid volume and signal intensity. For the next series of measurements, the same sample was re-melted at 403 K, quenched to 320 K, and measured during cooling in steps of 5 K down to 270 K (Figure 1, top panel). In this experiment, approximately half of the liquid crystallized when the temperature reached 290 K, reducing the signal intensity by half, but below 290 K, no further decrease of the signal intensity was observed, indicating no further crystallization on the timescale of measurement. Examining the sample at the end of experiment revealed red, orange, and yellow crystals embedded in an orange-red liquid.

Figure 2 shows the relaxation times τ_{HN} extracted from the loss curves. The filled circles are results obtained from measurements during heating and the empty circles, those during cooling (Figure 1). The solid line is the best fit to the VTF equation, $\log_{10}(\tau/s) = A + B/(T-T_0)$, where τ refers to τ_{HN} , $A = -20.7$, $B = 1904.6$ K and $T_0 = 175.4$ K. For this liquid, τ_{HN} approximately matches τ_{max} , the most probable relaxation time, and $\langle \tau \rangle$, the average relaxation time ($\tau_{\text{HN}}/\langle \tau \rangle = 1.44$). The kinetic glass transition temperature calculated from $\langle \tau \rangle = 100$ s is $T_g = 258.7$ K. This value is slightly smaller than 261 K, the onset temperature of the glass transition detected by DSC (heating at 10 K/min following cooling at 10

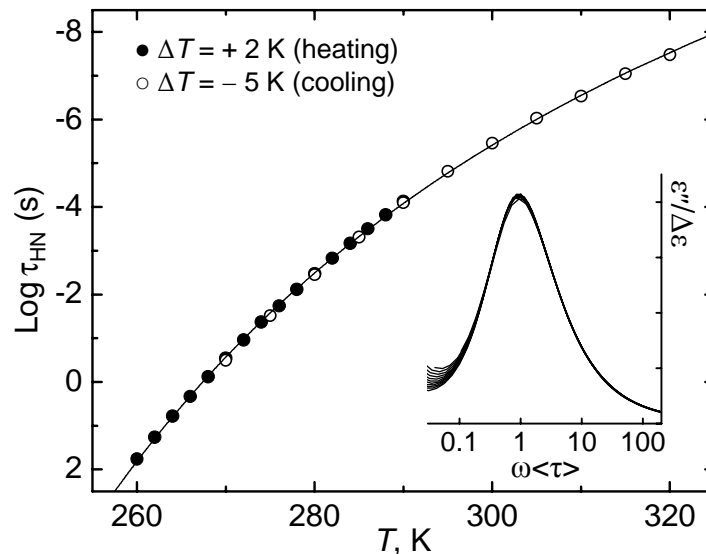


Figure 2. The dielectric relaxation time of liquid ROY vs. temperature. τ_{HN} extracted from the loss curves is shown. The filled circles are results from measurements during heating and the empty circles, those during cooling (Figure 1). The curve through the data points is the fit to the VTF equation, $\log(\tau/s) = A + B/(T-T_0)$, where $A = -20.7$, $B = 1904.6$ K, and $T_0 = 175.4$ K. The inset shows the normalized loss amplitude $\epsilon''/\Delta\epsilon$ vs. the normalized frequency $\omega\langle\tau\rangle$ across the τ range of 100 s to 100 ns. This overlay shows the temperature-time superposition symmetry of the liquid dynamics. These distribution curves are characterized by a constant β_{KWW} of 0.73.

K/min). The 2 K difference between the kinetic T_g and the calorimetric T_g is typical.²² The fragility index $m = d \log \langle \tau \rangle / d(T_g/T)|_{T=T_g}$ is 71. This m value classifies ROY as a fragile liquid; that is, its $\ln \langle \tau \rangle$ vs. $1/T$ relation deviates significantly from the Arrhenius law.

Because of the small differences between τ_{HN} , τ_{max} , and $\langle \tau \rangle$ relative to their large changes with temperature, we use τ_α to refer to them all. Across the viscous range ($\tau_\alpha = 100$ s - 100 ns), a constant stretching exponent $\beta_{KWW} = 0.73$ fits the relaxation spectra well. This constancy indicates that if displayed against $\log \nu$, the distribution of relaxation times does not broaden significantly as the temperature approaches T_g from above. Accordingly, a master curve can represent well all individual spectra once they are normalized to the same peak frequency and intensity (Figure 2, inset). This time-temperature superposition symmetry of liquid dynamics has been observed previously for TNB³² and OTP,²³ whose $\beta_{KWW} = 0.5$ is substantially smaller than that for ROY. In reference to the typical correlation between β_{KWW} and m ,²⁴ the value of the stretching exponent $\beta_{KWW} = 0.73$ is unexpectedly high given the fragility of liquid ROY. Such relatively narrow dispersions, however, have been reported for other highly polar systems and might be a consequence of significant correlations regarding the orientation of adjacent dipoles.²⁵

Figure 3 shows the data from an experiment performed to determine whether a secondary relaxation²⁶ exists in glassy ROY. A sample of ROY was quenched from 403 K to 120 K at 20 K/min and its ϵ'' vs. ν curve was measured during heating from 175 K to 280 K in steps of 5 K. The data show no well-defined β relaxation peak even at an amplitude 3.5 decades below that of the primary α relaxation. In another experiment, a ROY liquid was quenched from 403 K to 100 K at 490 K/min, a treatment that enabled the detection of a secondary relaxation peak of in glassy OTP.⁵ This experiment found no evidence for a secondary relaxation process in ROY. The lack of a conspicuous secondary process does not exclude the possibility that a secondary process might be hidden in the high-frequency wing of the primary relaxation peak.

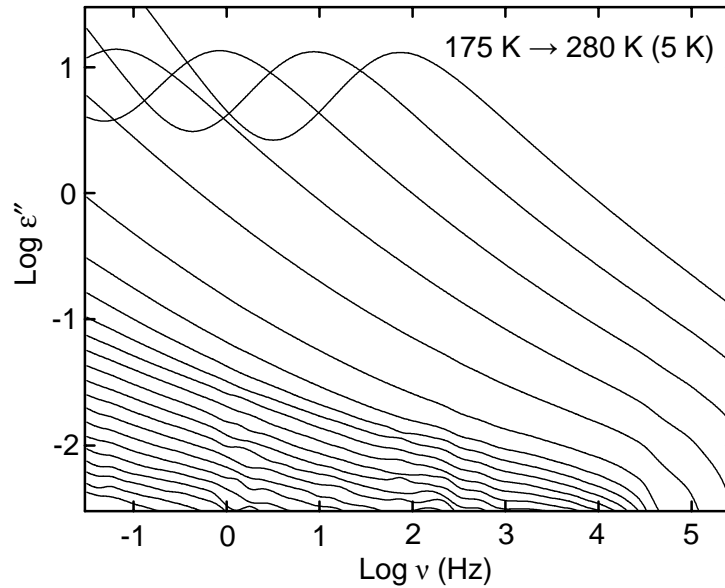


Figure 3. Dielectric loss ϵ'' vs ν at various temperatures. The measurements were made during heating from 175 to 280 K in steps of 5 K. No secondary (β) process could be detected.

Enthalpy Relaxation in the Glassy State. The kinetics of enthalpy relaxation of ROY glasses was measured by DSC. A ROY glass was prepared by cooling a liquid at 10 K/min to 248 K and annealing at 248 K for 0, 600, 1800, 3600, 7200, 14400, 21600, or 36000 s. After each annealing step, the glass was cooled at 10 K/min to 203 K and heated at 10 K/min to 403 K to measure its heat capacity C_p as a function of temperature (Figure 4a). By modulated DSC, the C_p of liquid ROY at 283 K was determined to be 1.57 J/(gK); the C_p curves obtained by standard DSC were shifted to this value. Figure 4a shows that the longer the aging time, the larger the enthalpy overshoot as the resulting glass transforms to the equilibrium liquid. The C_p change upon glass transition was found to be 0.43 J/(gK). This value changed insignificantly (± 0.01 J/(gK)) with the time of glass aging, which indicates that no significant crystallization occurred during aging.

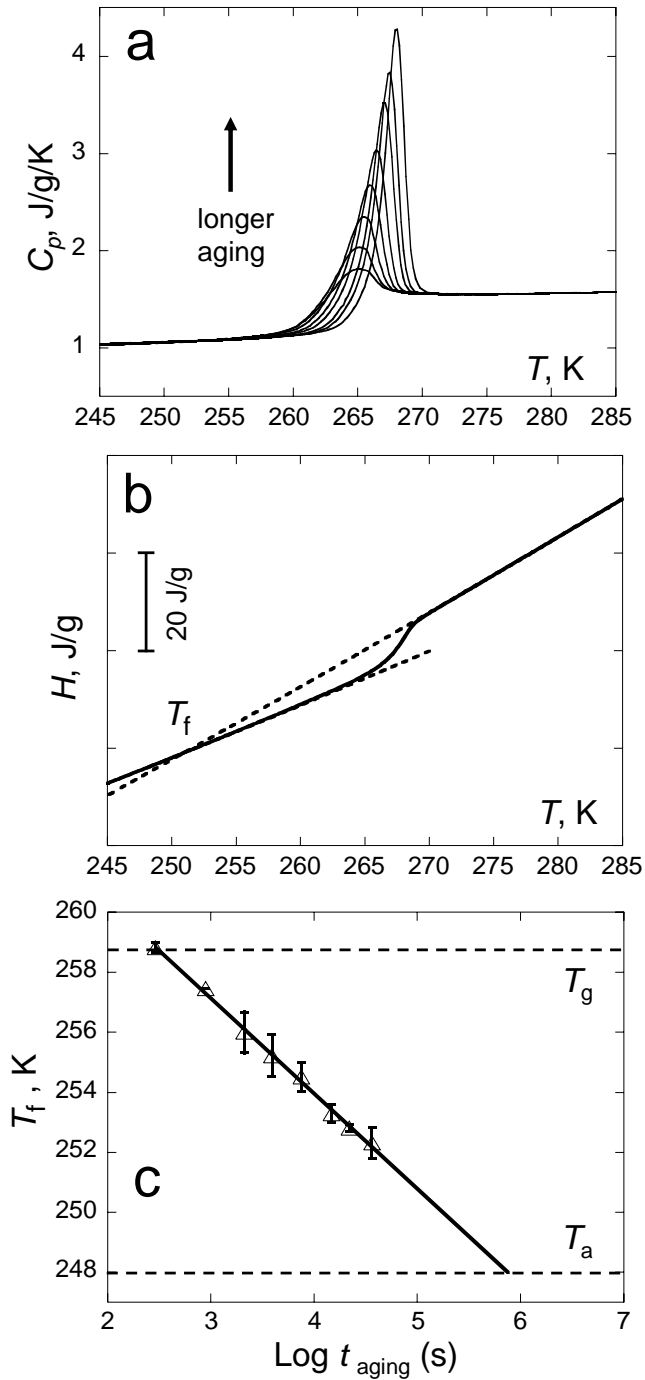


Figure 4. (a) C_p vs. T of ROY glasses aged at 248 K ($T_g - 11$ K) for 0, 600, 1800, 3600, 7200, 14400, 21600 and 36000 s. (b) Illustration of the determination of the fictive temperature T_f . Data is shown for a ROY glass aged at 248 K for 36000 s. (c) T_f of ROY glass vs. aging time t_{aging} at 248 K. T_g and T_a (aging temperature) are indicated as horizontal lines. The solid line is the linear fitting of the data. Each reported T_f was the average of three replicate measurements. 290 s was added to each isothermal aging time to account for glass relaxation before isothermal aging at 248 K.

We characterize the progress of glass relaxation using an enthalpic fictive temperature T_f , whose value ranges from T_g (no relaxation) to 248 K (full relaxation). Figure 4b shows how the T_f was calculated.²¹ The C_p is integrated to obtain the enthalpy of a glass relative to the equilibrium liquid and T_f is the

temperature at which the enthalpy of the equilibrium liquid extrapolated to below T_g intersects the enthalpy of the glass. For this calculation the C_p 's of the equilibrium liquid and the glass were fitted to linear functions and the resulting functions were extrapolated and integrated to yield the enthalpies needed to calculate T_f . The C_p data used for calculating the liquid enthalpy curve are chosen at temperatures sufficiently above T_g and those for calculating the glass enthalpy curve at temperatures sufficiently below T_g so that neither is affected by the enthalpy relaxation that occurs during the DSC heating. Extrapolating the glass enthalpy curve is necessary only if the aging time is short, which causes T_f to be close to T_g and the apparent glass enthalpy to be affected by relaxation during the DSC scan.

Figure 4c shows how the T_f of a freshly made glass decreases over time at 248 K. An initial aging time of $t_{a0} = 290$ s was added to each isothermal aging time to account for the glass relaxation that occurred while the material was cooled from T_g to T_a at 10 K/min. This small offset by t_{a0} does not alter the main feature of the T_f vs. t_a relation. To estimate t_{0a} , we first note that t_{0a} has a lower limit of 66 s, the time required to cool the sample from T_g to T_a at 10 K/min, because glass relaxation is expected to be faster above T_a than at T_a . Next we note that for long aging times, omitting t_{a0} would not introduce significant errors and that for long aging times, T_f was observed to vary approximately linearly with log (aging time): $T_f \approx a + b \log t$. Assuming that this relation holds also at shorter aging times and that the total aging time is equal to $(t_{a0} + t_a)$, we fitted the observed T_f vs. t_a data to $T_f = a + b \log (t_{a0} + t_a)$ and obtained $t_{a0} = 290$ s. Finally, we estimated t_{a0} from the dependence of T_f on cooling rate. The T_f of a glass formed by cooling at 5 K/min and no aging at 248 K approximately matched the T_f of a glass formed by cooling at 10 K/min and aging for 240 – 300 s at 248 K. Assuming that reducing the cooling rate from 10 to 5 K/min doubles t_{a0} , the t_{a0} for the 10 K/min cooling should lie between 240 and 300 s.

Figure 4c shows that at 248 K, the T_f of a freshly made ROY glass decreased by 7 K in 10 hours; in this time, the glass relaxes 60 % of the way towards the equilibrium liquid state. If this trend continued, it would take 10^6 s (12 days) for the T_f to reach 248 K, the aging temperature.

Time Dependence of GC Growth Rate. As crystals grow in the glassy state, the growth front meets a glass whose age depends on how long the growth front has been advancing. The further the growth front has advanced, the more aged the glass is before the crystal growth front. We studied whether this aging process causes a slowdown of a growth front over time. Figure 5 shows representative data of the distance advanced by polymorph YT04 vs. time; the slope of each curve is the growth rate. YT04 is the best polymorph for this study because of its smooth growth front. At 265 K ($T_g + 6$ K), the growth distance increases linearly with time and the growth rate is constant. In contrast, at 248 K ($T_g - 11$ K), the crystal growth slows slightly with time. The solid line through the 248 K data points is a linear fit of the data in the first 14400 s; the subsequent data points fall significantly below the line. The decrease of growth rate at 248 K is (13 ± 3) % in 10 h (based on 3 measurements) and 34 % in 30 h (based on one measurement).

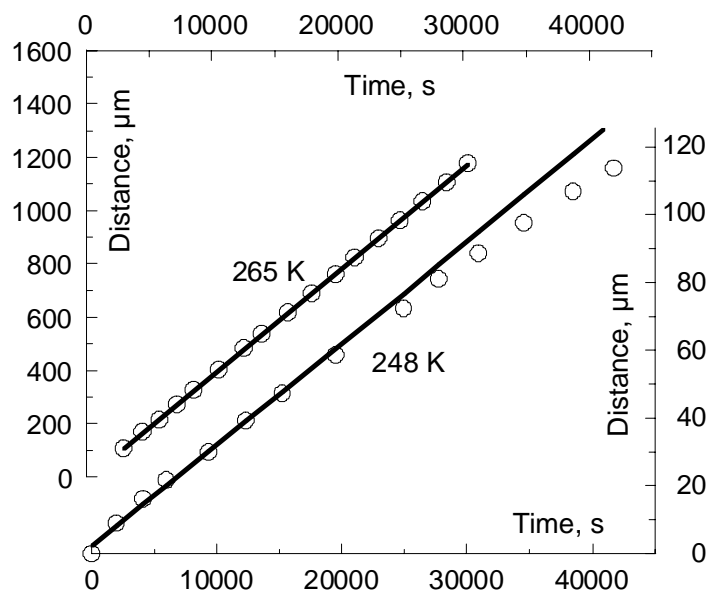


Figure 5. Growth of YT04 polymorph in the GC mode at 265 and 248 K. At 265 K, the growth rate is constant over the time of observation (30000 s); the line is the linear fit of the entire data. At 248 K, the growth rate decreases slightly over time; the line is the linear fit of the first 14400 s of data.

To increase experimental throughput, growth-ring experiments were performed to study the time dependence of crystal growth rate. Figure 6a (inset) shows an example of YT04 growth rings. The bright rings grew at 265 K; the three dark rings grew at 248 K in 14400, 28800, and 57600 s (left to the right). Figure 6 shows the average growth rates over three consecutive time intervals at 265 K (0 – 7200 s, 7200 – 14400 s, and 14400 – 28800 s) and at 248 K (0 – 14400 s, 14400-28800 s, and 28800-57600 s). The time intervals are indicated by the horizontal arrows and each error bar represents the standard deviation of at least 5 measurements. The data show that the average growth rate does not change significantly at 265 K, but decreases significantly at 248 K. The slowdown of crystal growth observed using the growth ring method is consistent with that observed in real time.

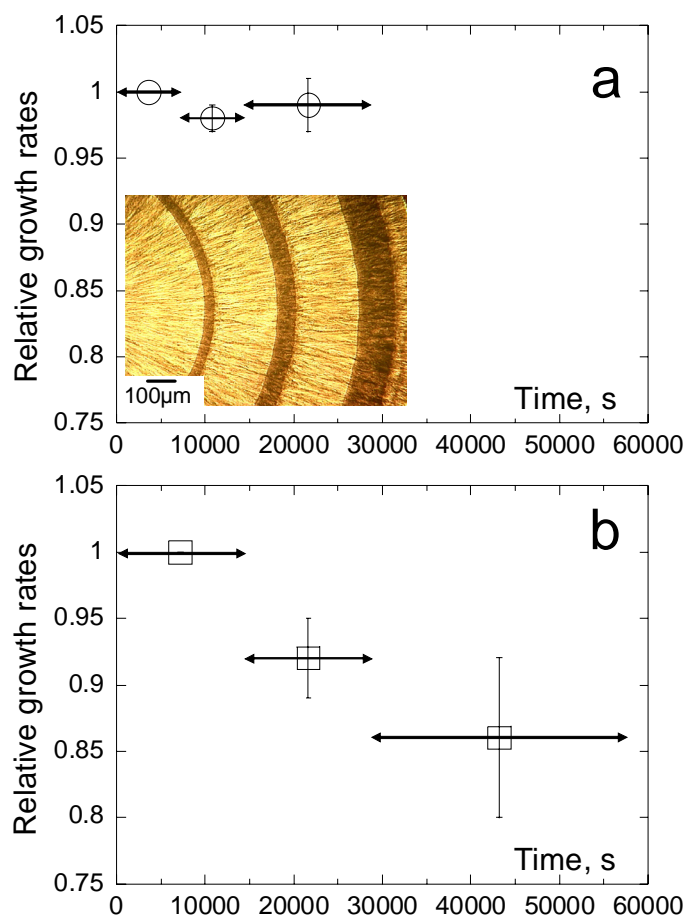


Figure 6. Growth rates of YT04 polymorph (a) at 265 K averaged over the first 7200 s, next 7200 s, and next 14400 s and (b) at 248 K averaged over the first 14400 s, next 14400 s, and next 28800 s. In both panels, growth rates are normalized to the growth rate in the initial time interval. Error bar is standard deviation of at least 5 measurements. Inset: Growth rings developed at 265 K (bright) and 248 K (dark).

DISCUSSION

Growth of ROY Polymorphs under and Free from Control by Bulk Diffusion. The primary dielectric relaxation time τ_α of a liquid has been found to represent accurately the timescale of structural relaxation and molecular rotation.²⁷

In Figure 7 we compare the τ_α of liquid ROY with the characteristic time for crystal growth, τ_u , defined as the time required for the crystalline phase to gain one molecular layer: $\tau_u = a/u$, where a is the molecular diameter and u is the crystal growth rate. Figure 7a displays the τ_u 's for all the polymorphs whose growth has been measured near T_g ;¹⁶ Figure 7b displays the τ_u 's for only two polymorphs, ON and YT04, to represent the polymorphs that do not and do exhibit GC growth.

Figure 7a shows that for the polymorphs not showing the GC mode (ON, YN, and R05), the growth rate is generally characterized by $\tau_u > \tau_\alpha$. One exception to this relation is the lowest-temperature data point for YN, though the difference between

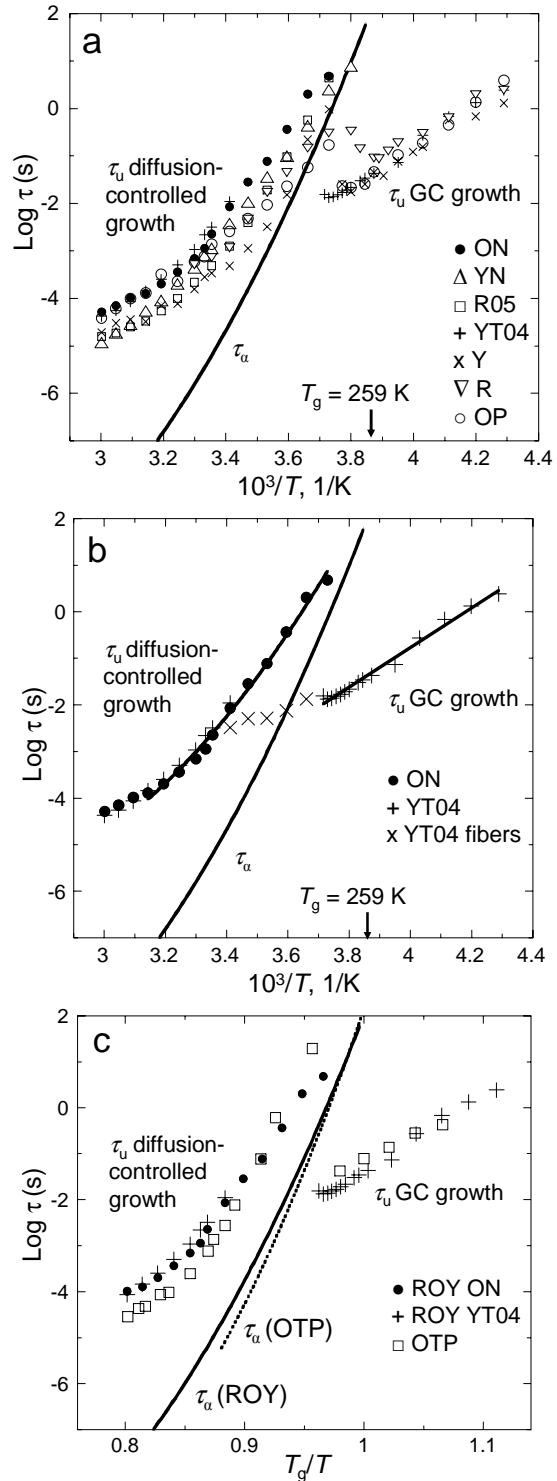


Figure 7. Comparison of the timescales of liquid relaxation and crystal growth. τ_u is the time required for the crystal to grow one molecular layer: $\tau_u = a/u$, where a is the molecular diameter and u is the crystal growth rate. (a) displays the τ_u 's for seven ROY polymorphs. (b) shows the τ_u 's for ON and YT04 to represent the polymorphs not showing and showing GC growth. In (c) the τ_u vs. τ_α relation of ROY is compared against that of OTP wherein T is scaled by T_g .

τ_u and τ_α is probably not experimentally significant. Figure 7a also shows that for these polymorphs, τ_u has weaker temperature dependence than τ_α .

To study the relation between τ_u and τ_α for the polymorphs not showing GC growth, we plot them against each other in the log-log format (Figure 8). For this plot, we have made a small correction of τ_u so that only the kinetic part of the crystal growth rate is correlated with the liquid dynamics. The revised τ_u , or $\tau_{u,kin}$, is given by a/u_{kin} , where $u_{kin} = u/[1 - \exp(-\Delta G/RT)]$. In the last equation, ΔG is the free-energy difference between the liquid and the crystalline phases and calculated from the temperature and heat of melting of the ROY polymorphs.^{17,18} u_{kin} thus calculated represents the kinetic part of the crystal growth rate, or the growth rate achievable if the thermodynamic driving force were infinity. This thermodynamic correction is significant near the crystal's melting point (ΔG is small), but relatively small near T_g (ΔG is large and $[1 - \exp(-\Delta G/RT)]$ approaches unity).

Figure 8 shows that the $\log \tau_{u,kin}$ vs. $\log \tau_\alpha$ plots are approximately linear for ROY polymorphs over decades of change. The data points fall above the dashed line defined by $\tau_{u,kin} = \tau_\alpha$ with the exception of

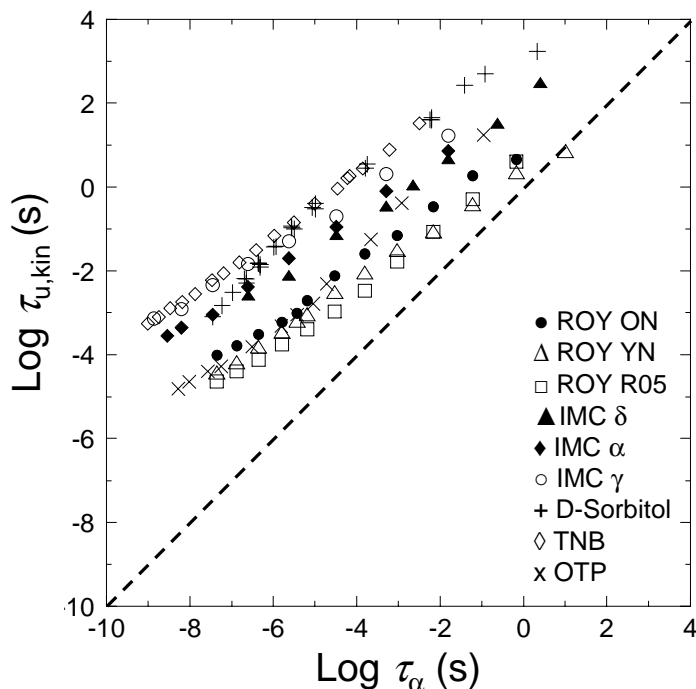


Figure 8. $\log \tau_{u,kin}$ vs. $\log \tau_\alpha$ plots for diffusion-controlled crystal growth in ROY and other liquids. $\tau_{u,kin} = a/u_{kin}$, where a is the molecular diameter and u_{kin} is the kinetic part of the crystal growth rate. The slope yields the exponent in the power-law relation $\tau_{u,kin} \propto \tau_\alpha^\xi$. $\xi = 0.69$ for ON, 0.67 for YN, and 0.73 for R05.

that for YN at the lowest temperature of measurement as noted above. The slope of each plot (ξ) is significantly less than unity: $\xi = 0.69$ for ON, 0.67 for YN, and 0.73 for R05. Thus, a power-law relation exists between $\tau_{u,\text{kin}}$ and τ_{α} : $\tau_{u,\text{kin}} \propto \tau_{\alpha}^{\xi}$, with $\xi \approx 0.7$. Figure 8 also shows that a similar relation exists for other organic liquids: OTP, 1,3-bis(1-naphthyl)-5-(2-naphthyl)benzene [commonly called tris(naphthylbenzene) or TNB], D-sorbitol, and indomethacin (IMC; 3 polymorphs). For these plots the τ_{α} has also been obtained by dielectric spectroscopy. Table 1 collects the corresponding ξ values. All the liquids are organic liquids with comparable fragilities.

Table 1. Value of ξ in the power-law relation between crystal growth rate and dielectric relaxation time $\tau_{u,\text{kin}} \propto \tau_{\alpha}^{\xi}$

System	$a, \text{\AA}^a$	T_g, K^b	T/T_g range	$\xi(\text{R}^2)^c$	References
ROY YN	7.5	259	1.01-1.23	0.65(0.998)	u (16); τ_{α} (this work)
ROY ON			1.03-1.23	0.69(0.994)	
ROY R05			1.03-1.23	0.73(0.993)	
IMC δ	8.5	316	1.03-1.18	0.72(0.996)	u (28); τ_{α} (29)
IMC α			1.06-1.18	0.68(0.999)	
IMC γ			1.06-1.18	0.65(0.994)	
D-sorbitol	6.6	268	1.00-1.23	0.83(0.988)	u (28,30); τ_{α} (5)
TNB	9.7	345	1.08-1.24	0.75(0.999)	u (31); τ_{α} (32)
OTP	7.7	243	1.04-1.28	0.84(0.983)	u (33); τ_{α} (5)

^a Molecular diameter.

^b Temperature at which $\langle \tau \rangle = 100$ s or if $\langle \tau \rangle$ is unavailable, $\tau_{\text{max}} = 100$ s.

^c R^2 is the correlation coefficient of fitting.

The relation $\tau_{u,\text{kin}} \propto \tau_{\alpha}^{\xi}$ is reminiscent of a previously observed relation between u_{kin} and viscosity η : $u_{\text{kin}} \propto \eta^{-\xi}$, where $\xi \approx 0.7$.³⁴ For the same liquid, the ξ values obtained from the two correlations are comparable (within 0.1). The two relations of course anticipate each other if τ_{α} scales with η^{-1} . Yet another relation pertinent to the present discussion is the fractional Stokes-Einstein relation that applies to fragile liquids near T_g : $D \propto \eta^{-\xi}$, where ξ is again close to 0.7. It has been argued that the similarity between $u_{\text{kin}} \propto \eta^{-\xi}$ and $D \propto \eta^{-\xi}$ indicates that the diffusion coefficient D more accurately describes the temperature dependence of u_{kin} than the viscosity η . This supports the designation of the crystal growth kinetics in these liquids as diffusion-controlled.

Figure 7a shows that in contrast to ON, YN, and R05, polymorphs YT04, Y, OP, and R grow so much faster near and below T_g that the corresponding τ_u can be many orders of magnitude shorter than τ_α and that τ_u has a much weaker temperature slope than τ_α . These properties justify the description of the growth of these polymorphs as not under diffusion control or “diffusionless”. This designation is appropriate not only for the fully activated GC mode, which yields compact spherulites, but also the growth of loose fibers above T_g (“x” in Figure 7b), which have been assigned as the precursors of GC growth in the equilibrium liquid.⁸

Figure 7c compares the characteristic times of crystal growth and dielectric relaxation in liquid ROY and liquid OTP near T_g . For this comparison the temperature has been normalized by T_g . For OTP, the τ_u is calculated from the crystal growth rates from Magill and Li (for diffusion-controlled growth)³³ and from Xi et al. (for GC growth)¹⁵ and the τ_α data are from Wagner and Richert.⁵ Figure 7c shows that the two systems are remarkably similar in the way crystal growth transitions from a diffusion-controlled mode to the GC mode near T_g .

Why Does Crystal Growth in Glassy ROY Slow with Time? This study found that the rate of GC growth u in liquid ROY is constant at 265 K ($T_g + 6$ K), but slows slightly with time at 248 K ($T_g - 11$ K). At 248 K, u decreases by ca. 13 % in 10 hours, which is in contrast with previous reports that the growth rate is independent of time.^{2,3,7} During this time, the ROY glass undergoes substantial relaxation (ca. 60 %) toward the equilibrium liquid (Figure 4c). Because the time dependence of u is pertinent to understanding the fast crystal growth from glasses, we consider here a few possible reasons for the decrease of u at 248 K. We find that none of the effects considered explains well this phenomenon.

One way to distinguish the crystal growth at 248 K and 265 K is to envision that at 265 K ($T_g + 6$ K), the growth front enters a liquid that has been equilibrated (the liquid’s τ_α is 4 s at 265 K), whereas at 248 K ($T_g - 11$ K), the growth front enters a glass that is undergoing relaxation and whose structure has less or more time to evolve, depending on whether the growth front meets it earlier or later. At the beginning of a measurement, the glass before the growth front is “freshly made” with $T_f \approx 259$ K (T_g);

after the growth has gone on for 10 hours, the glass before the growth front has had the same time to relax and attained a T_f of 252 K (Figure 4).

We consider first whether the slowdown of GC mode crystal growth could result from the effect of glass aging on the thermodynamic driving force of crystallization. The free energy of a glass is expected to decrease with aging, reducing the driving force of crystallization. In making this statement, we assume of course that free energy (an equilibrium property) is meaningfully defined for a glass (a non-equilibrium system). If the glass aging at temperature T reduces its fictive temperature from T_{f1} to T_{f2} , the free-energy decrease may be estimated from

$$G_{g2} - G_{g1} = \Delta C_p [T_{f2} - T_{f1} - T \ln (T_{f2}/T_{f1})] \quad (2)$$

where ΔC_p is the heat capacity difference between a glass and the equilibrium liquid ($\Delta C_p = 111$ J/K/mole for ROY). Eq. 2 is derived by considering a thermodynamic cycle that connects the glass of T_{f1} and the glass of T_{f2} via the supercooled liquid. The derivation assumes that ΔC_p is independent of temperature and the same for the two glasses of different fictive temperatures. Note again that the validity of Eq. 2 depends on the validity of applying equilibrium thermodynamics to a relaxing system.

By this calculation, the free energy of a freshly made ROY glass decreases by 21 J/mole after 10 hours of aging at 248 K. This amount is small relative to $\Delta G \approx 6$ kJ/mole, the thermodynamic driving force of crystallization at 248 K for the supercooled liquid. Assuming the crystal growth rate varies with ΔG in the manner proposed by Wilson and Frenkel,^{10,11}

$$u = u_{kin} \{1 - \exp[-\Delta G/(RT)]\} \quad (3)$$

the slowdown of crystal growth would be 0.06 %, much smaller than the 13 % slowdown observed.

The calculation just made allows an estimate of the effect of aging on the vapor pressure of a ROY glass. Using the equation,

$$\ln \left[\frac{p_g(T_{f2}, T)}{p_g(T_{f1}, T)} \right] = \frac{G_{g2} - G_{g1}}{RT} \quad (4)$$

we find that aging a freshly made ROY glass at 248 K for 10 hours decreases its vapor pressure by 1 %. This decrease could be expected to lead to the same decrease of the escaping tendency of molecules from a ROY glass.³⁵ The observed 13 % slowdown of GC growth rate therefore cannot be explained by the loss of escaping tendency of molecules by aging.

We next consider how aging affects the rate of structural relaxation in a ROY glass. According to the Adam-Gibbs-Vogel (AGV) equation,³⁶ the structural relaxation time increases with aging:

$$\log \tau_a = A + \frac{B}{T(1 - T_0/T_f)} \quad (5)$$

where A , B , and T_0 are the VTF parameters that characterize the structural relaxation in the equilibrium liquid and T_f is the fictive temperature of the glass of interest. This model assumes that the α relaxation time of a glass is that given by the Adam-Gibbs model wherein the configurational entropy is replaced by the value of the equilibrium liquid at the fictive temperature. To implement this calculation, we assume the VTF parameters are given by our dielectric measurement and the T_f is given by our calorimetric measurement (Figure 4c). By this calculation, τ_a increases by 23 times in 10 hours of aging at 248 K (Figure 9). This increase is much greater than the 13 % deceleration of GC growth under the same condition, indicating GC growth is largely decoupled from the structural relaxation of

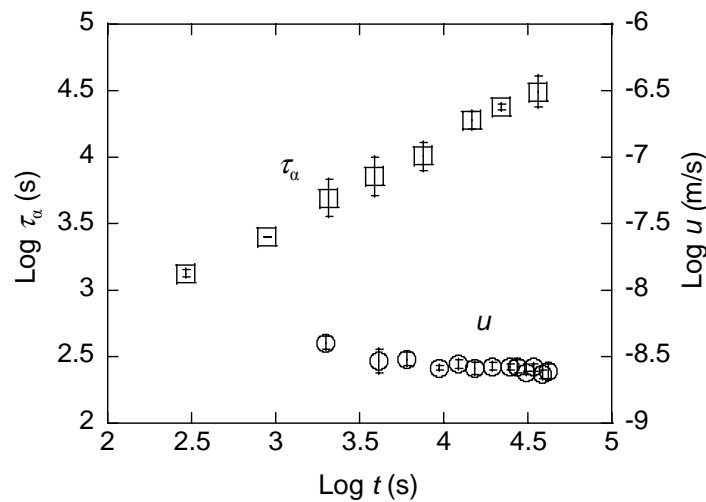


Figure 9. Comparison of the time dependences of the glass τ_a calculated using eq. 5 and the GC mode crystal growth rate u at 248 K. In 10 hours, the growth rate decreases by 13 % while the glass τ_a increases by 23 times.

the glass. These different time dependences support the notion already established with data collected above T_g , namely, that GC growth is not controlled by the α relaxation.

In summary, the slowdown of GC growth in glassy ROY over time is not readily explained by the decrease of the thermodynamic driving force of crystallization, the decrease of glass vapor pressure, or the slowdown of structural relaxation.

Is GC Growth Related to a Secondary (β) Relaxation? It has been proposed that a secondary (β) relaxation might provide the molecular motions responsible for GC growth.^{37,16} This view is sensible because while the primary (α) relaxation is largely quenched in a glass, a secondary relaxation is still observable in many glass formers.²⁶ This view has the merit that a secondary relaxation generally has a shorter characteristic time than GC growth ($\tau_\beta < \tau_u$) and similar activation energy as GC growth. Yet another support for this view is the analogy between the separation of τ_u near $1.15 T_g$ into diffusion-controlled and GC branches and the α - β bifurcation envisioned for liquid dynamics.²⁶

A previous study of liquid OTP¹⁵ found, however, that the observation of a well-defined secondary relaxation process by dielectric spectroscopy is not required for observing GC growth. This conclusion is reached because even after a secondary relaxation peak disappears upon glass relaxation,⁵ GC growth is still observable in glassy OTP. Whatever molecular motions give rise to this secondary relaxation peak of OTP, those motions are apparently irrelevant to GC growth. The present study supports this conclusion. Because liquid ROY exhibits no secondary relaxation peak and yet shows GC growth, the existence of a secondary relaxation peak is not a necessary condition for observing GC growth. Among the glass formers now known to exhibit GC growth, toluene shows a secondary relaxation peak even upon aging,³⁸ OTP shows a short-lived secondary relaxation peak,⁵ and ROY shows no secondary relaxation peak. It should be noted that a conspicuous peak of secondary relaxation is likely only one manifestation of molecular motions in glasses; there could be other secondary processes (perhaps detectable with other techniques) that could be associated with GC growth.

CONCLUSIONS

We studied the liquid dynamics of 5-methyl-2-[(2-nitrophenyl)amino]-3-thiophenecarbonitrile, named ROY for its red, orange, and yellow crystal polymorphs, with dielectric spectroscopy and differential scanning calorimetry to understand the fast, diffusionless growth of some but not all of its polymorphs. We found ROY to be a typical fragile organic liquid. Its α relaxation process has the time-temperature superposition symmetry across the viscous range ($\tau_\alpha = 100$ s - 100 ns) with the width of the relaxation peak characterized by a constant β_{KWW} of 0.73. No secondary relaxation peak was observed, even with glasses made by fast quenching. For the polymorphs not showing fast growth in the glassy state, the growth rate has a power-law relation with τ_α , $u \propto \tau_\alpha^{-\xi}$, where $\xi \approx 0.7$, and the time required for the crystal to gain one molecular layer substantially exceeds τ_α . The growth of these polymorphs is reasonably described as diffusion-controlled. For the polymorphs showing fast crystal growth in the glassy state, the growth is so fast near and below T_g that during one τ_α , thousands of molecular layers can be added to the crystalline phase and the growth rate “decouples” from τ_α to a much greater extent. This mode of crystal growth is not controlled by bulk diffusion. When occurring in the glassy state, this mode of growth slows slightly over time, as has been reported for glassy *o*-terphenyl. This slowdown is not readily explained by the effect of physical aging on the thermodynamic driving force of crystallization, the decrease of glass vapor pressure, or the rate of structural relaxation.

ACKNOWLEDGMENT We thank the NSF-funded UW MRSEC and NSF (DMR-0804786) for supporting this work.

REFERENCES

- 1 Zallen, R. *The Physics of Amorphous Solids*. John Wiley & Sons, New York, 1983.
- 2 R. J. Greet, D. J. Turnbull, Chem. Phys. **46**, 1243 – 1251 (1967).
- 3 T. Hikima, Y. Adachi, M. Hanaya, M. Oguni, Phys. Rev. B **52**, 3900 (1995).
- 4 Mapes, M. K.; Swallen, S. F.; Ediger, M. D. J. Phys. Chem. B **2006**, 110, 507-511.
- 5 Wagner, H.; Richert, R. J. Phys. Chem. B **1999**, 103, 4071-4077.
- 6 M. Hatase, M. Hanaya, M. Oguni, J. Non-Cryst. Solids **333**, 129-136 (2004).
- 7 T. Konishi, H. J. Tanaka, Phys. Rev. B, **76**, 220201(R) (2007).
- 8 Sun, Y.; Xi, H.; Ediger, M. D.; Yu, L. J. Phys. Chem. B. **112(3)**, 661-664 (2008).
- 9 Ishida, H.; Wu, T.; Yu, L. J. Pharm. Sci. **96**, 1131-8 (2007).
- 10 H. A. Wilson, Phil. Mag. **50**, 238 – 251 (1900).
- 11 J. Frenkel, Physik Z. der Sowjet Union **1**, 498 – 500 (1932).
- 12 W. B. Hillig, D. Turnbull, J. Chem. Phys. **24**, 914 (1956).
- 13 Uhlmann, D. R.; Uhlmann, E. V. In *Nucleation and Crystallization in Liquids and Glasses*. Weinberg, M.C., Ed.; The American Ceramic Society: Westerville, OH (1993).
- 14 Ngai, K. L.; Magill, J. H.; Plazek, D. J. J. Chem. Phys. **112**, 1887-1892 (2000).
- 15 Xi, H.; Sun, Y.; Yu, L. J. Chem. Phys. **130**, 094508-1 to 094508-9 (2009).
- 16 Sun, Y.; Xi, H.; Chen, S.; Ediger, M. D.; Yu, L. J. Phys. Chem. **112**, 5594-5601 (2008).

-
- 17 Yu, L.; Stephenson, G. A.; Mitchell, C. A.; Bunnell, C. A.; Snorek, S. V.; Bowyer, J.; Borchardt, T. B.; Stowell, J. G.; Byrn, S. R. *J. Am. Chem. Soc.* **122**, 585-591 (2000).
- 18 Chen, S.; Guzei, I. A.; Yu, L. *J. Am. Chem. Soc.* **127**, 9881 (2005).
- 19 Havriliak, S.; Negami, S. *Polymer* **8**, 101 (1967).
- 20 Alvarez, F.; Alegria, A.; Colmenero, J. *Phys. Rev. B* **44**, 7306 (1991).
- 21 C. T. Moynihan, S. K. Lee, M. Tatsumisago, T. Minami, *Thermochimica Acta* **280/281**, 153-162 (1996).
- 22 L.-M. Wang, Y. Tian, R. Liu, R. Richert, *J. Chem. Phys.* **128**, 084503 (2008)
- 23 Richert, R. *J. Chem. Phys.* **123**, 154502/1-154502/3 (2005).
- 24 Böhmer, R.; Ngai, K.L.; Angell, C.A.; Plazek, D.J. *J. Chem. Phys.* **99**, 4201 (1993).
- 25 Nielsen, A.I.; Christensen, T.; Jakobsen, B.; Niss, K.; Olsen, N.B.; Richert, R.; Dyre, J.C. *J. Chem. Phys.* **130**, 154508 (2009).
- 26 G. P. Johari, M. Goldstein, *J. Chem. Phys.* **53**, 2372-88 (1970).
- 27 Ediger, M. D.; Angell, C. A.; Nagel, S. R. *J. Phys. Chem.* **100**, 13200-13212 (1996).
- 28 Wu, T.; Yu, L. *J. Phys. Chem. B* **110**, 15694-15699 (2006).
- 29 Carpentier, L.; Decressain, R.; Desprez, S.; Descamps, M. *J. Phys. Chem. B* **110**, 457-464 (2006).
- 30 Yu, L. *Cryst. Growth & Design* **3**, 967-971 (2003).
- 31 Magill, J.H.; Plazek, D. J. *J. Chem. Phys.* **46**, 3757-3769 (1967).
- 32 Richert, R.; Duvvuri, K.; Duong, L.-T. *J. Chem. Phys.* **118**, 1828-1836 (2003).

-
- 33 Magill, J.H.; Li, H. M. J. Crystal Growth **20**, 135-44 (1973).
- 34 Ediger, M. D.; Harrowell, P.; Yu, L. J. Chem. Phys. **128(3)**, 034709/1-034709/6 (2008).
- 35 I. Langmuir, Phys. Rev. **11**, 329 – 342. (1913)
- 36 I. M. Hodge, J. Non.-Cryst. Solids **169(3)**, 211-66 (1994).
- 37 T. Hikima, M. Hanaya, M. Oguni, J. Non-Cryst. Solids **235-237**, 539 (1998).
- 38 S. A. Lusceac, C. Koplin, P. Medick, M. Vogel, N. Brodie-Linder, C. LeQuellec, C. Alba-Simionesco, E. A. Roessler, J. Phys. Chem. B **108**, 16601-16605 (2004).